Evaluation of stiffness derivative for a delta wing with straight leading edges in unsteady flow

Renita Sharon Monis, Asha Crasta, S.A. Khan

Abstract— The emphasis of this paper is to examine the Stiffness derivative variation with the pivot position by varying Mach number in unsteady flow and its comparison with quasi-steady flow of Crasta & Khan for varying angle of attack with different Mach number. From the results, it is evident that Stiffness derivative decreases as the Mach number increases. Comparison with Liu as well as Crasta & Khan theory it is evident that there is an improvement in the present theory being unsteady over quasi-steady theory, in addition to the fact that in the present work the pressure on the leeward surface is taken into account which results in increased value of the stability derivative and the same is clearly visible in results.

Keywords: Delta wing, Hypersonic, Straight leading edge, Unsteady.

INTRODUCTION

Ghosh [1] has developed a 2D large deflection hypersonic similitude. The resulting piston theory is not restricted to slender shapes as in the cases of Lighthill's [2] and Miles [3] piston theories. Ghosh's piston theory has been applied (Ghosh et al. [4]) to oscillating plane ogives to predict C_{m_q} .The similitude was extended to non-slender cones/quasi cones, and a new kind of piston motion, called conico-annular piston motion was given by Ghosh [5]. Oscillating delta wings at large incidence was treated by Ghosh [6].

According to Liu & Hui [7] depending on the combination of flight Mach number, the angle of attack, the ratio of specific heats of the gas and the swept back angle of the wing for an oscillating triangular wing in supersonic/hypersonic flow the shock wave may be attached or detached from the leading edges.

Etkin [8] and Levin [9] have shown the separate effects of the pitch rate and incidence rate on the pitching moment. Hui et al. [10] have studied the problem of stability of an oscillating flat plate wing of arbitrary plan form placed at a specified mean angle of attack in supersonic/hypersonic flow by applying strip theory. The plane piston theory of Ghosh was applied with the inclusion of wave reflection effect to obtain in closed form $C_{m_{\dot{\alpha}}}$ for non-slender wedges/plane ogives in Hypersonic flow (Ghosh et al. [11]).

Ghosh [12] has given a unified hypersonic similitude, and a consequent piston theory which is valid for wedges/quasi-wedges for any Mach number greater than 1 and $E \leq 0.3$ provided bow shock is attached. It is assumed that at each spanwise station, the flow is 2-D with the shock attached. To assess the overall stability the moment derivatives due to the pitch rate as well as incident rate should be evaluated. In the present work, the unified similitude of Ghosh [14] along with the extended theory of Crasta & Khan is combined with strip theory to obtain the unsteady moment derivative for the delta wing with the straight leading edge.

In this paper, an attempt has been made to study the Stiffness derivative with different pivot position which gives the better comparison with the theory developed by Liu as well as Crasta & Khan.

Implemented two-dimensional slender body theory in supersonic/hypersonic flow at the high angle of attack for various Mach number by utilizing the concept of piston theory, relations for stability derivatives were obtained for a wedge, which depends on the flight Mach number and semi vertex angle of the wedge [16]–[23].

The theory developed by Crasta and Khan [24]-[25] which is a quasi-steady can now be extended to unsteady theory to predict the formulae for Stiffness derivative.

Khan et al., [26] analytical and numerical methods are used to evaluate flow over a wedge at supersonic Mach numbers. Closed form solutions are obtained for the various semi-vertex angle of the wedge and the Mach numbers

Renita et al., [27] an analytical study to account the effect of the sweep angle of a delta wing

whose leading edges are curved on roll damping derivative at various angles of attack and the amplitude of the full sine waves?

Musavir et al., [28] simulated the trajectory of the unguided rolling projectiles at varying Mach numbers using aerodynamic coefficients. The aerodynamic coefficients are estimated using an aerodynamic prediction code, Missile DATCOM. The predicted stability derivatives will determine the design criteria, and also their effect on the design aspects (stability and accuracy) of the projectile. To satisfy the condition of stability for the trajectory of the projectile, a model of 6 DOF equations has been used.

The boundaries of periodic, quasiperiodic, and chaotic motions were obtained to ascertain whether roll–pitch

Revised Version Manuscript Received on February 14, 2019.

Renita Sharon Monis, Assistant Professor (Sr.), SMVITM, Bantakal & Research Scholar, MITE, Moodbidri, Mangalore, Karnataka, India, (Email: renita.maths@sode-edu.in)

Asha Crasta, Assosciate Professor, MITE, Moodbidri, Mnagalore, Karnataka, India, (Email:asha@mite.ac.in)

S.A. Khan, Department of Mechanical Engineering, Faculty of Engineering, International Islamic University, Kuala Lumpur, Malaysia, (E-mail: sakhan06@gmail.com)

resonance lock-in occurs through phase portrait analysis, and to activate roll breakout by controlling the rotation number [29].

A mathematical model of a projectile with wraparound fins is solved numerically using the Runge-Kutta-Fehlberg scheme for various values of the control parameter. An analysis of the dynamic variables has been performed using the time history of signals, phase portraits, Poincare sections, power spectrum estimation, etc. [30].

ANALYSIS

The equations that govern the flow in the similitudinal plane in the region between the shock and the surface of the oscillating equation become

$$\frac{\partial \rho}{\partial \tau}+\frac{\partial(\rho v)}{\partial \bar{y}}=0$$

$$\rho\left(\frac{\partial}{\partial \tau}+v\frac{\partial}{\partial \bar{y}}\right)v+\frac{\partial p}{\partial \bar{y}}=0$$

$$\left(\frac{\partial}{\partial \tau}+v\frac{\partial}{\partial \bar{y}}\right)\ln\left(\frac{p}{\rho^{\gamma}}\right)=0$$

(1) - (3)

Where ρ is the density, p is the pressure, v is the velocity component in the $\bar{y}$ direction and τ is the time which is measured from the instant the fluid slab reaches the leading edge of the wedge. According to Ghosh [14] unified similitude, the velocity of the flow in the slab is independent of the motion of the fluid of other parallel slabs.

Let the perturbations in velocity and pressure immediately behind the shock be denoted by $\bar{v}_s$ and $\bar{p}_s$ respectively. These perturbations are due to unsteady waves originating at the body surface and catching up with the shock. This leads to perturbation $\bar{V}_0$ in the shock velocity. The linear expressions that are obtained in a straight forward manner by perturbing the shock wave Rankine-Hugoniot relations, relating these perturbation quantities are

$$\frac{\bar{p}}{\rho_2 a_2 v_2}=G_0\frac{\bar{V}_0(\frac{\xi}{\alpha})}{V_0}+H_0\frac{\bar{V}_0(\frac{\eta}{\beta})}{V_0} \qquad (4)$$

$$\frac{\bar{V}}{V_2}=G_0\frac{\bar{V}_0(\frac{\xi}{\alpha})}{V_0}-H_0\frac{\bar{V}_0(\frac{\eta}{\beta})}{V_0} \qquad (5)$$

On simplifying (4) and noting that for higher Mach numbers, when $\cos\bar{\phi}\approx 1$ and $\bar{\psi}\approx\delta$ we get the same expression as Ghosh et al. [11] which is

$$\bar{P}_p=\rho_2 a_2 U_\infty\left[C_1\theta+C_2\frac{\dot{\theta}x}{U_\infty}+C_3\frac{\dot{\theta}L}{U_\infty}\right]$$

Where

$$C_1=\left(\frac{1+w}{1-w}\right)\frac{\cos\delta}{\cos\phi}$$

$$C_2=\left(\frac{1}{\cos\phi}+\frac{\cos\delta}{\cos\phi}\right)\left(\frac{1+w\delta'}{1-w\delta'}\right)-\left(\frac{1+w}{1-w}\right)\frac{\cos\delta}{\cos\phi}$$

$$C_3=-\left(\frac{1+w}{1-w}\right)\frac{k}{\cos\phi} \qquad (6)$$

For the windward side, we have

$$-\frac{\partial M}{\partial\theta}=\rho_2 a_2 u_\infty c_1 L^2\left(\frac{1}{2}-k\right) \qquad (7)$$

It should be noted that the upper surface is at a much lower pressure than the windward surface. It will be shown that the contribution to damping at large Mach number is negligible as compared to that of the windward side.

Piston Mach number

$$M_p=\frac{V_p}{a_e}=\frac{M_e\theta}{\cos\mu_e}+\frac{(x-kL)\dot{\theta}}{a_e\cos\mu_e} \qquad (8)$$

Where Me is the Mach number downstream of the expansion fan, a_e is the sonic velocity and μ_e is the Mach angle downstream of Prandtl-Meyer expansion.

The isentropic expression for pressure ratio is given by

$$\frac{P_p}{P_e}=\left(1-\frac{\gamma-1}{2}M_p\right)^{\frac{2\gamma}{\gamma-1}} \qquad (9)$$

As $\theta\to 0$

$$\frac{P_p}{P_e}\approx 1-\gamma M_p \qquad (10)$$

The pitching moment is given by

$$\bar{M}=\int_0^L (x-kL)P_p\,dx \qquad (11)$$

$$-\frac{\partial\bar{M}}{\partial\theta}=\frac{p_\theta\gamma M_\theta L^2}{\cos\mu_e}\left(\frac{1}{2}-k\right) \qquad (12)$$

The total effect of both the windward and leeward surface is, therefore,

$$-\frac{\partial\bar{M}}{\partial\theta}=\rho_2 a_2 u_\infty c_1 L^2\left(\frac{1}{2}-k\right)+\frac{p_e\gamma M_e L^2}{\cos\mu_e}\left(\frac{1}{2}-k\right) \qquad (13)$$

Ghosh [10] in his theory invokes strip theory, which can be applied if $\tan r_1 << 1$ or $\tan\phi.AR^{-1}<<1$ where is the shock standoff angle at the leading edge and AR is the aspect ratio. For hypersonic Mach number <<1 so that . According to Ghosh's [12] unified similitude, a further restriction is

Published By:
Blue Eyes Intelligence Engineering
& Sciences Publication

necessary such that where is the axial component of the Mach number behind the bow shock. Consider a delta wing with the arbitrary straight leading edge at large mean angle of incidence whose geometry is shown below.

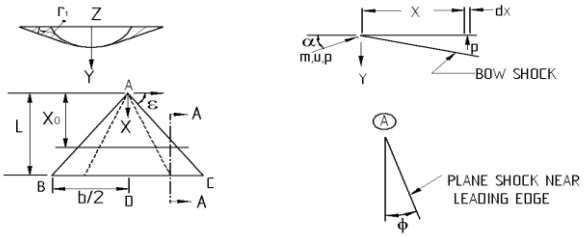

The equation to the straight leading edge is

$$Z = x\cot\varepsilon$$

Wing area = $L^2\cot\varepsilon$

AR = b^2/wing area= $4\cot\varepsilon$ (14)

Where $b = 2L\cot\varepsilon$

Stiffness derivative is given by,

$$-C_{m_\theta} = \frac{1}{\frac{1}{2}\rho_\infty U_\infty{}^2 L^3\cot\varepsilon}\left(-\frac{\partial\bar{M}}{\partial\theta}\right) \quad (15)$$

At any span-wise location, we have,

$$-\left(\frac{\partial\bar{M}}{\partial\theta}\right)_1 = \rho_2 a_2 u_\infty c_1 L_1{}^2\left(\frac{1}{2}-k_1\right)+\frac{p_e\gamma M_e L_1{}^2}{\cos\mu_e}\left(\frac{1}{2}-k_1\right) \quad (16)$$

Where L1 is the local chord length and k1 is the local non-dimensional pivot position.

$$L_1 = L - x$$

$$k_1 = \frac{x_0 - x}{L - x} = \frac{l - x + x_0 - L}{L - x} = 1 - \frac{L(1-k)}{L - x}$$

$$k = \frac{x_0}{L} \quad (17)$$

For the complete wing $-\frac{\partial\bar{M}}{\partial\theta}$ is given by,

$$-\frac{\partial\bar{M}}{\partial\theta} = \int\left(-\frac{\partial M}{\partial\theta}\right)_1 dz \quad (18)$$

On simplification we get,

$$-\frac{\partial\bar{M}}{\partial\theta} = -\frac{A_1 L^3\cot\varepsilon}{3} + A_1 L^3(1-k)\cot\varepsilon$$

where

$$A_1 = \rho_2 a_2 U_\infty C_1 + \frac{p_\theta\gamma M_e}{\cos\mu_e} \quad (19)$$

Using the equations from (1) to (19) we derive the expression for stiffness derivative as

$$-C_{m_\theta} = 4\left(\frac{1}{3}-\frac{k}{2}\right)\left\{\frac{C_1\sin\psi}{M}+\frac{P_e}{P_\infty}\frac{M_e{}^2}{M_\infty{}^2}\frac{1}{\sqrt{M_e{}^2-1}}\right\}$$

It is assumed that the pressure perturbation is the same for a flat plate oscillating in a stream of Mach number M_e at zero angles of attack. By this approach oscillation of expansion fan due to the plate, oscillation is neglected. Noting that the upper surface is at a much lower pressure than the windward surface.

$$-C_{m_\theta} = 4\left(\frac{1}{3}-\frac{k}{2}\right)\left\{\frac{C_1\sin\psi}{M}\right\}$$

Based on the above theory, results are obtained for various geometrical, and inertia parameters, and the same has been discussed.

RESULTS AND DISCUSSION

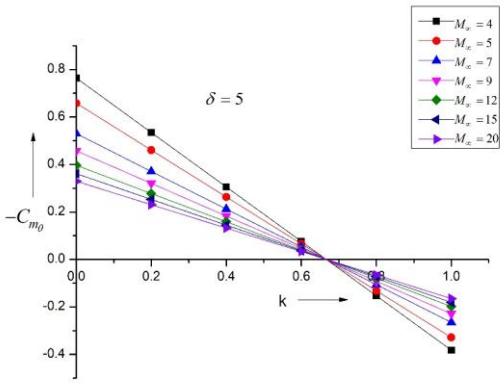

Figure.1: Stiffness derivative versus pivot position for δ = 5.

Figure1 presents Stiffness derivative variation with pivot position for $\delta = 5^0$. As Mach number increases the stiffness derivative due to pitch, continue to decrease. From the figure, it is found that there is an increase of 13.9 % in the pitching moment coefficient for the inertia increment from 4 to 5. Its magnitude continues to vary for a different range of the Mach number. This increase is 19.5 % for Mach from Mach 5 to 7. Similarly, there is an increase in the stiffness derivative of 13.6 % for Mach 7 to 9, 13.4 % for Mach 9 to 12, 8.8 % for Mach 12 to 15, and 8.9 % Mach 15 to 20. The reasons for this variation in decrement is the pressure distribution on the surface of the wing, its variation along the chord and the variation of the inertia levels. It is expected that for lower Mach the decrement will be large in the stiffness derivative as compared to a very high value of the Mach number where the flow has attained a steady-state, and it remains constant. After that, there is no much difference due to the Mach number independence principle.

Published By:
Blue Eyes Intelligence Engineering
& Sciences Publication

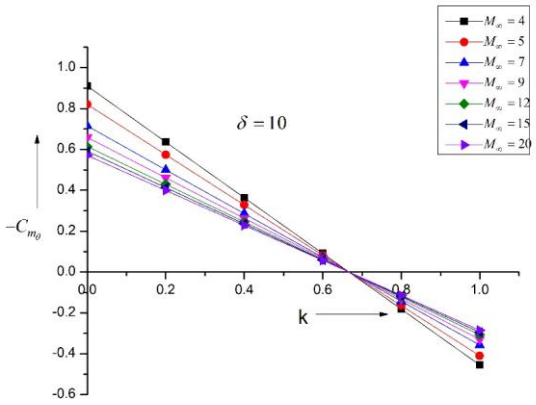

Figure.2: Stiffness derivative versus pivot position for δ = 10.

Fig. 2 represents Stiffness derivative variation with pivot position for $\delta = 10^0$. As Mach number increases the stiffness derivative due to pitch, continue to decrease. From the figure, it is found that there is an increase of 9.8 % in the pitching moment coefficient for the inertia increment from 4 to 5. Its magnitude continues to vary for a different range of the Mach number. This increase is 12.9 % for Mach from Mach 5 to 7. Similarly, there is an increase in the stiffness derivative of 7.9 % for Mach 7 to 9, 6.8 % for Mach 9 to 12, 3.8 % for Mach 12 to 15, and 3.3 % Mach 15 to 20. The magnitude of the stiffness derivative is reduced due to the increment in the flow deflection angle. The reasons for this variation in the stiffness derivative are due to the change in the pattern of the pressure on the surface of the wing.

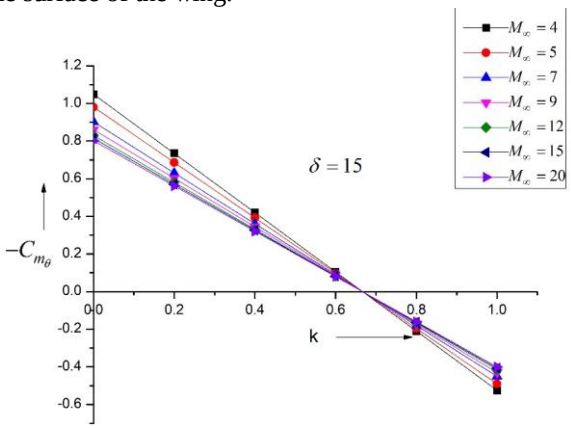

Figure.3: Stiffness derivative versus pivot position for δ = 15.

Fig. 3 presents Stiffness derivative variation with pivot position for $\delta = 15^0$. As Mach number increases the stiffness derivative due to pitch, continue to decrease. From the figure, it is found that there is an increase of 6.6 % in the pitching moment coefficient for the inertia increment from 4 to 5. Its magnitude continues to vary for a different range of the Mach number. This increase is 8.1 % for Mach from Mach 5 to 7. Similarly, there is an increase in the stiffness derivative of 4.5 % for Mach 7 to 9, 3.6 % for Mach 9 to 12, 1.8 % for Mach 12 to 15, and 1.6 % Mach 15 to 20. From the figure, it is seen that due to the further increase in the delta has resulted in a decrease in the stiffness derivative due to the larger planform area of the wing.

Fig. 4 presents Stiffness derivative variation with pivot position for $\delta = 20^0$. As the angle delta is further increased, there is further decrement in the stiffness derivative due to pitch. From the figure, it is found that there is an increase of 3.9 % in the pitching moment coefficient for the inertia increment from 4 to 5. Its magnitude continues to vary for a different range of the Mach number. This increase is 4.8 % for Mach from Mach 5 to 7. Similarly, there is an increase in the stiffness derivative of 2.5 % for Mach 7 to 9, 1.9 % for Mach 9 to 12, 1.01 % for Mach 12 to 15, and 0.78 % Mach 15 to 20. From the figure, it is seen that the flow deflection angle of twenty degrees is not advisable and it seems that shock wave is no more attached with the vertex point of the wing.

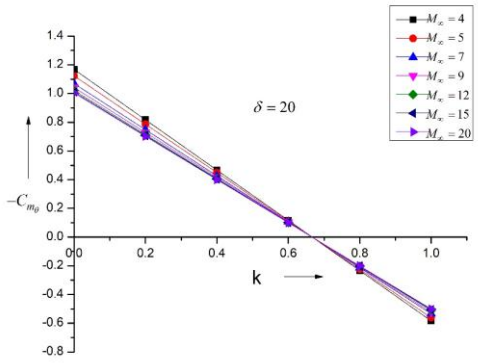

Figure.4: Stiffness derivative versus pivot position for δ = 20.

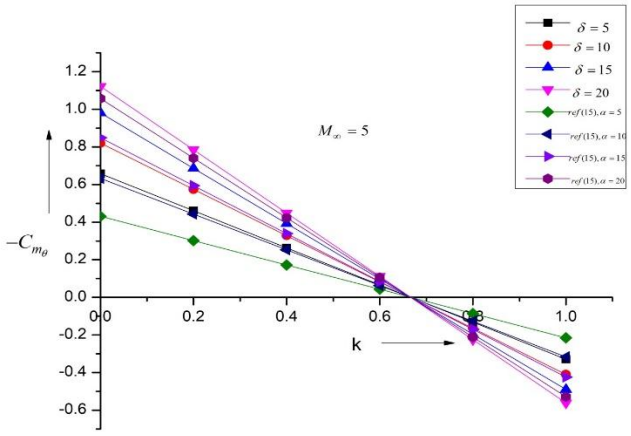

Figure 5: Stiffness derivative versus pivot position for $M_\infty = 5$.

Stiffness derivative vs. pivot position (h) is shown in Fig. 5 for Mach 5. These results indicate that the magnitude of the stiffness derivatives is more significant than that of Ref. (15). It is found that for a flow deflection angle of five degrees, the

magnitude of the stiffness derivative is thirty-four percent larger than Ref. (15). Similarly, for ten degrees, fifteen degrees, and twenty degrees, the magnitude of stability derivatives are more significant by twenty-three percent, fourteen percent, and six percent. The reasons for this discrepancy may be due to the present theory being unsteady, whereas the theory of Ref. (15) is quasi-steady. This also proves that the results obtained from the present theory are accurate as compared to the methods of Ref. (15). Further, it is seen that when the flow deflection angle is increased from five to ten degrees, there is around twenty percent, whereas when the flow deflection angle is increased from ten to fifteen degrees and fifteen to twenty degrees the increase in the stiffness derivative due to the pitch is in the range sixteen and twelve percent. The increase in the stability derivative is due to the increase in the plan form area, of the wing, and this results in an increase in the aspect ratio of the wing. It is well known that the lift curve slope of the wing will increase with the increase of the aspect ratio.

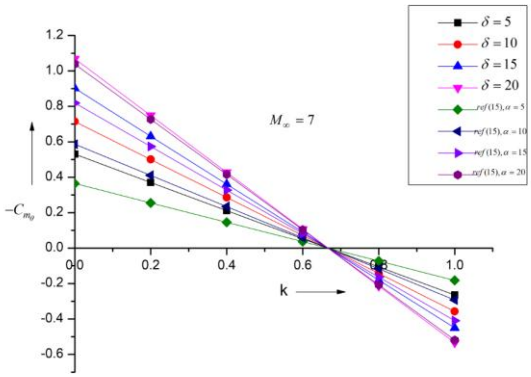

Figure 6: Stiffness derivative versus pivot position for M = 7.

Fig. 6 presents the results of stiffness derivatives at Mach M = 7 for a range of the flow deflection angles from five degrees to twenty degrees. From the previous case, there is a marginal increase in the inertia level as the Mach number is increased from 5 to 7. The figure indicates that with the increase in the flow deflection angle from five to ten, ten to fifteen and fifteen to twenty degrees, there is the increase in the stiffness stability derivative by twenty-six percent, twenty-one percent, and sixteen percent. These increments in the stability derivatives are attributed to the increase in the span of the wing and hence, the aspect ratio. When these results are compared with the Ref. (15) for the same range of the flow variables, it is found that the magnitude of the stability derivatives are higher as compared to those obtained by Ref. (15), and these increased values are thirty-one percent, eighteen percent, nine percent, and three percent when these values are compared for flow deflection angles of five, ten, fifteen, and twenty degrees.

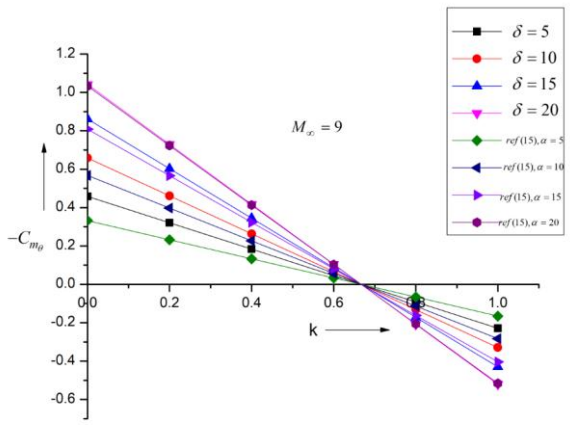

Figure 7: Stiffness derivative versus pivot position for M = 9.

With further increase in the Mach number from M = 7 to 9, the results of the stiffness derivatives are shown in Fig. 7 for flow deflection angles in the range from five to twenty degrees at a step of five degrees. Due to the increase in the angle δ and hence the planform area of the wing results in enhancement of the stability derivatives in the range thirty percent, twenty-four percent, and seventeen percent for the increase in the flow deflection angles from five to ten degrees, ten to fifteen degrees, and from fifteen to twenty degrees. Similarly, the difference in the stability derivatives obtained by the present theory and with that from Ref. (15), the increase in the stiffness derivative is twenty-eight percent, fourteen percent, six percent and 1 percent for flow deflection angles from five degrees to twenty degrees at an interval of five degrees.

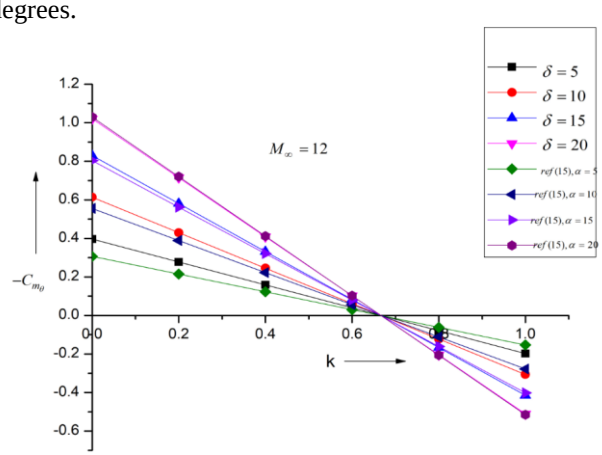

Figure 8: Stiffness derivative versus pivot position for M = 12.

With further increase in the Mach number from M = 9 to 12, the results of the stiffness derivatives are shown in Fig. 8 for flow deflection angles in the range from five to twenty degrees at a step of five degrees. Due to the increase in the

angle δ and hence the planform area of the wing results in enhancement of the stability derivatives in the range thirty six percent, twenty-six percent, and nineteen percent for the increase in the flow deflection angles from five to ten degrees, ten to fifteen degrees, and from fifteen to twenty degrees. Similarly, the difference in the stability derivatives obtained by the present theory and with that from Ref. (15), the increase in the stiffness derivative is twenty-two percent, ten percent, three percent and negative one percent for flow deflection angles from five degrees to twenty degrees at an interval of five degrees. This trend may be due to the increase in the Mach number where the Mach number independence principle comes into effect.

When there is an increase in the Mach number from M = 12 to 15, the results of the stiffness derivatives are shown in Fig. 7 for flow deflection angles in the range from five to twenty degrees at a step of five degrees. Due to the increase in the angle δ and hence the planform area of the wing results in enhancement of the stability derivatives in the range thirty nine percent, twenty-eight percent, and nineteen percent for the increase in the flow deflection angles from five to ten degrees, ten to fifteen degrees, and from fifteen to twenty degrees. Similarly, the difference in the stability derivatives obtained by the present theory and with that from Ref. (15), the increase in the stiffness derivative is nineteen percent, seven percent, two percent and minus two percent for flow deflection angles from five degrees to twenty degrees at an interval of five degrees.

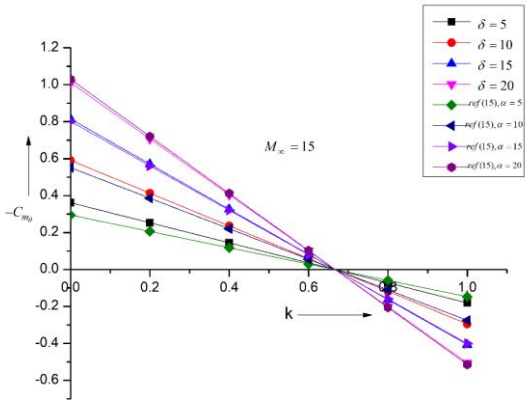

Figure 9: Stiffness derivative versus pivot position for M = 15.

Results at Mach M = 15 are shown in Fig. 9. In view of the increase in the Mach number, the dependency of the stability derivative with the Mach number is no more visible. At such a high Mach number, the flow variable becomes independent of the inertia levels. Further, it is seen that there is a continuous increase in the magnitude of the stiffness derivatives when the flow deflection was increased from five to ten degrees, ten to fifteen degrees, and fifteen to twenty degrees. The percentage increment in the stiffness derivatives is thirty-nine, twenty-eight, and nineteen percent. It is also seen that the magnitude of stiffness derivative obtained by contemporary theory is more significant than obtained by Ref. [15] as the present theory is fully unsteady and also accounts for the effect of the lee surface and Ref. [15] does not consider.

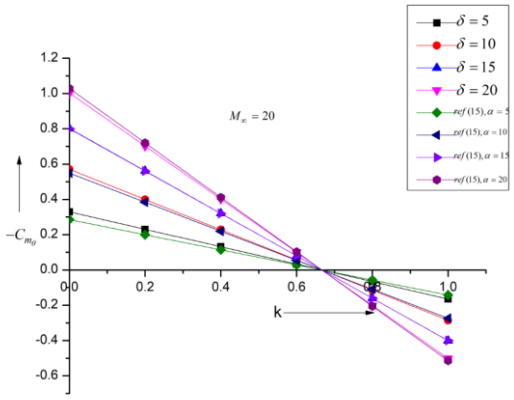

Figure 10: Stiffness derivative versus pivot position for M = 20.

Fig. 10 shows the results of stiffness derivatives when the Mach number is increased from M = 15 to 20; when the flow deflection angles are in the range from five to twenty degrees at a step of five degrees. Due to the increase in the angle δ and hence the planform area of the wing results in enhancement of the stability derivatives in the range forty-two percent, twenty-nine percent, and twenty percent for the increase in the flow deflection angles from five to ten degrees, ten to fifteen degrees, and from fifteen to twenty degrees. Similarly, the difference in the stability derivatives obtained by the present theory and with that from Ref. (15), the increase in the stiffness derivative is fourteen percent, four percent, all most zero percent and negative three percent for flow deflection angles from five degrees to twenty degrees at an interval of five degrees.

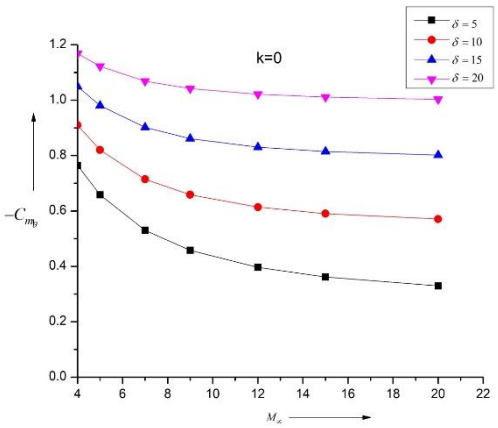

Figure 11: Stiffness derivative versus Mach No. for pivot Position k = 0.

Figure11 shows the graph of Stiffness derivative versus Mach number at the nose of the wing. It is seen that the value of Stiffness derivative is near to 0.8, 0.9, 1.05, 1.18 at Mach M = 5 for various flow deflection angles δ = 50, 100, 150, and 200. The increase in flow deflection angle results in sixteen percent, thirteen percent, and ten percent enhancement in the stability derivative due to the pitch. This linear increase in the

stiffness derivative is due to the change in the geometrical parameter. Due to the increase in parameter δ, there is an increase in the planform area of the wing resulting in pressure distribution of the wing leading to increase in the span of the wing and hence, increase in the lift generated by the delta wing. For the same change in the geometrical variables at Mach M = 5, the percentage increase in the stability derivatives is in the range twenty percent, sixteen percent, and thirteen percent. When we observe the results at Mach M = 7, their magnitudes are in the range twenty-six percent, twenty-one percent, and sixteen percent. Similarly, at Mach M = 9, 12, and 15, they are in the range from thirty to thirty-nine percent, twenty-four to twenty-eight percent, and seventeen to nineteen percent.

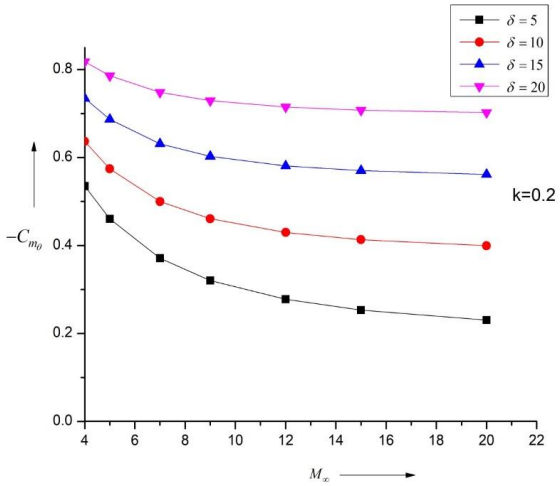

Figure 12: Stiffness derivative versus Mach No. for pivot Position k = 0.2

Fig. 12 presents results of stiffness derivative due to the pitch for pivot position k = 0.2, which twenty percent away from the nose and has moved towards the trailing edge. It is seen that for a flow deflection angle of five degrees results in a minimum value, later with the increase in the flow deflection angle the magnitude increases and the increase varies from twenty to twelve percent. For all the values of the flow deflection angle for Mach M = 12 and above the stiffness derivative becomes independent of Mach number.

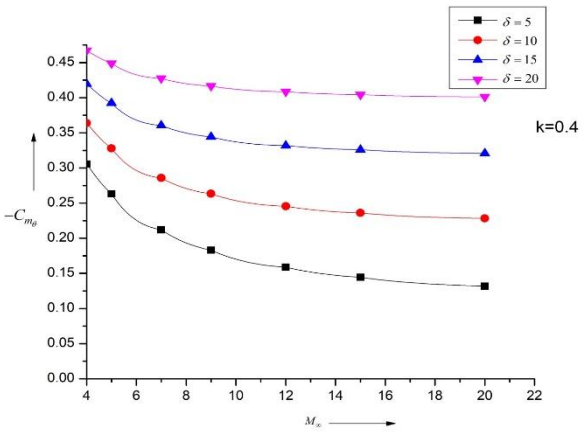

Figure 13: Stiffness derivative versus Mach No. for pivot Position k = 0.4

Results for Pivot position of k = 0.4 are shown in Fig. 13. Results indicate that there is a further decrease in the values of the stiffness derivative and the values vary from thirty percent to seventeen percent. This decrease in the values of the stability derivative is attributed to the shift of the pivot position resulting in totally different pressure field and hence the pitching moment. Mach number independence principle is applicable for Mach M = 12 and above.

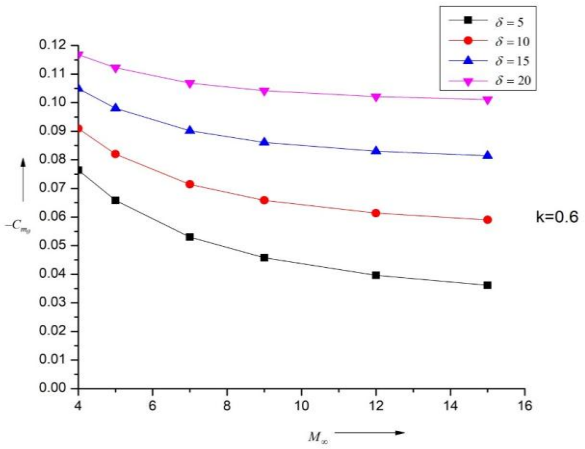

Figure 14: Stiffness derivative versus Mach No. for pivot Position k = 0.6

With the further shift in the pivot position towards the trailing edge, the results for k = 0.6 are shown in Fig. 14. In view of the further shift in the pivot position, there is a further decrease in the stability derivatives. The variation is from thirty to nineteen percent for the high range of the parameters. The Mach number independence principle still holds for Mach M = 12 and above.

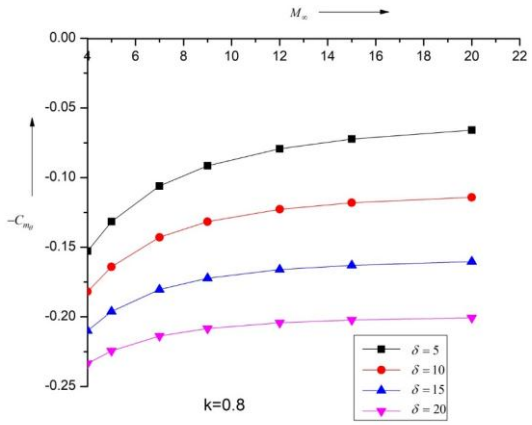

Figure 15: Stiffness derivative versus Mach No. for pivot Position k = 0.8

Fig. 15 presents the results for pivot position k = 0.8. For this case, the values are too low and have become cynical. This location is far away from the leading edge and very close to the trailing edge. As above for Mach M = 12 and above the values remained constant and independent of Mach number.

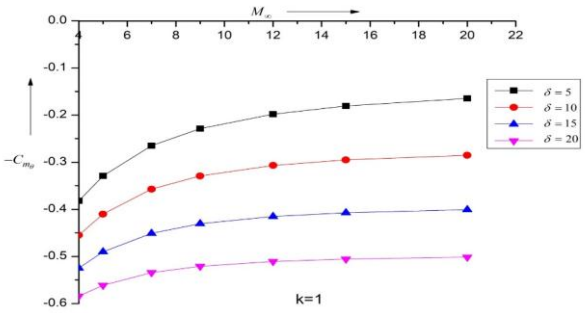

Figure 16: Stiffness derivative versus Mach No. for pivot Position k = 1.0

Fig. 16 shows the results for pivot position of k = 1.0 which is located at the trailing edge. As discussed earlier, the Mach number independence takes place for M = 12 and above.

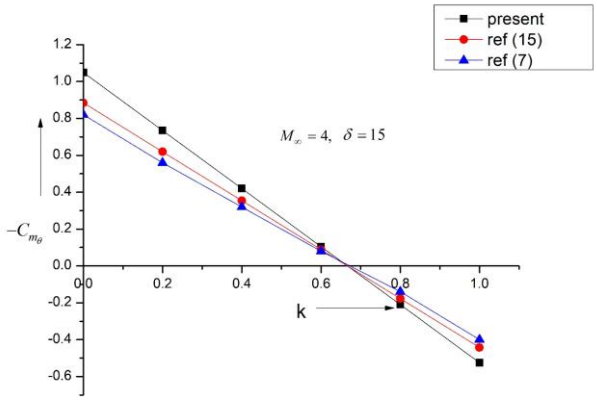

Figure 17: Stiffness derivative versus pivot position for Mach No. 4.

In Fig. 17 results of stiffness derivatives computed by the present theory are compared with Ref. [7] and [15]. From the results, it is seen that percentage increase between Ref. [15] and the present theory at different pivot positions in the range from 0 to 1 are around nineteen percent. When we compare the results of the present theory with Ref. [7], they are twenty-eight, thirty-one, fifty percent, and the difference between Ref. [7] and Ref. [15] the percentage in the range from eight percent, eleven percent, and twenty-six percent. The present theory is fully unsteady, whereas that of Ref. [7] and Ref. [15] are quasi and unsteady. The magnitude of the stiffness derivative for the present theory is the maximum, followed by Ref. [15] and then Ref. [7]. Ref. [15] even though fully unsteady but still, the magnitude is lower than the present theory as they have neglected the effect of lee surface.

CONCLUSIONS

From the above discussions, we can draw the following conclusions:

1. The Stiffness derivative decreases with Mach number and increases with the flow deflection angle.

2. The present theory is fully unsteady, whereas that of Ref. [7] and Ref. [15] are quasi and unsteady. The magnitude of the stiffness derivative for the present theory is the maximum, followed by Ref. [15] and then Ref. [7]. Ref. [15] even though fully unsteady but still, the magnitude is lower than the present theory as they have neglected the effect of lee surface.

3. The Stiffness derivative decreases for the different pivot position with Mach number whereas, it continues to increase with the angle of attack.

4. For the pivot position of k = 0.6 all the graph they intersect at the same point; which is nothing but the point where the center of pressure will be located. This shows that the center of pressure for all the cases remains the same.

5. It is found that with the increase of Mach number there is a decrease in the stiffness derivative, and later it is independent of Mach number.

REFERENCES

1. Ghosh, K.,1977, "A New Similitude for Aerofoils in Hypersonic Flow," Proceedings of the 6th Canadian Congress of Applied Mechanics, Vancouver, Canada, May 29-June 3, pp. 685-686.
2. Light Hill, M.J., 1953, "Oscillating Aerofoil at High Mach Numbers," Journal of Aeronautical Sciences, Vol. 20, June, pp. 804-812.
3. Miles, J.W., 1960, "Unsteady flow at hypersonic speeds, Hypersonic Flow," Butterworth's Scientific Publications, London, pp. 685-686.
4. Ghosh K. and Mistry B. K., 1980, "Large incidence Hypersonic Similitude and Oscillating Non-planar Wedges," AIAA Journal, Vol. 18, Issue 8, Aug. pp. 1004-1006.
5. Ghosh, K. 1984, "Hypersonic Large Deflection Similitude for Quasi wedges and Quasi-cones," Aeronautical Journal, March, pp.70-76.
6. Ghosh, K. 1984, "Hypersonic Large Deflection Similitude for oscillating delta wings," Aeronautical Journal, Oct., pp. 357-361
7. Lui, D. D and Hui, W. H., 1977, "Oscillating delta wings with attached shock waves," AIAA Jr., June, pp. 804-812.
8. Etkin, E., 1972, "Dynamics of atmospheric flight," Wiley, New York.
9. Levin, D.A., 1984, "Vortex lattice method for calculating longitudinal dynamic Stability derivatives of oscillating delta wings," AIAA Journal, January, pp. 6-12.
10. Hui W. H. et al., 1982, "Oscillating Supersonic/Hypersonic wings at High Incidence," AIAA Journal, Vol. 20. Issue 3, March, pp. 299-304.
11. Ghosh, K., Vempathi and Das, D.1985, "Hypersonic flow past non-slender wedges, cones and ogives in oscillation," The Aeronautical Journal, August, pp. 247-256.
12. Ghosh, K., 1986, "Unified supersonic/hypersonic similitude for oscillating wedges and plane ogives," AIAA Journal, Vol. 24, No. 7, July, pp. 1205-1207.
13. Hui, W.H., 1969, "Stability of oscillating wedges and caret wings in hypersonic and supersonic flows," AIAA Journal, Vol. 7, No. 8, August, pp.1524-1530.
14. Ghosh K, 1983, "Unified similitude for wedge and cone with attached shock," extended abstract published in Canadian Congress of Appl. Mechanics, University of Saskatchewan, Saskatoon, Canada , May 31-June 3, pp. 533-544.

15. Asha Crasta and Khan S. A, 2012, "Oscillating Supersonic delta wing with Straight Leading Edges," International Journal of Computational Engineering Research, Vol. 2, Issue 5, September, pp. 1226-1233.
16. S. Pavithra, M. Bashir, S. Lavanya, and S. A. Khan, "Estimation of Stability Derivatives in Pitch for an Oscillating Wedge in Hypersonic Flow," Advances and applications in fluid mechanics, vol. 19, no. 4, pp. 873–882, 2017.
17. R. S. Monis, A. Shabana, A. Crasta, and S. A. Khan, "Computation of Stiffness derivative for an unsteady delta wing with curved leading edges," International Journal of Recent Research, vol. 4, no. 4, pp. 71–74, 2017.
18. A. Shabana, R. S. Monis, A. Crasta, and S. A. Khan, "Estimation of Stability derivative of an Oscillating cone in Hypersonic Flow," International Journal of Recent Research, vol. 4, no. December, pp. 46–52, 2017.
19. S. Pavitra, S. Lavanya, and S. A. Khan, "Estimation of Stability Derivatives of wedges at Supersonic Mach Numbers," no. December 2017, 2018.
20. S. Pavitra, S. Lavanya, and S. A. Khan, "Stability derivatives of oscillating wedges in viscous hypersonic flow," IOP Conference Series: Materials Science and Engineering, vol. 370, p. 012051, 2018.
21. A. Shabana, R. S. Monis, A. Crasta, and S. A. Khan, "Computation of Stability Derivatives of an oscillating cone for specific heat ratio = 1.66," IOP Conference Series: Materials Science and Engineering, vol. 370, p. 012059, 2018.
22. Shabana, R. S. Monis, A. Crasta, and S. A. Khan, "Estimation of Stability Derivatives in Newtonian Limit for Oscillating Cone," IOP Conference Series: Materials Science and Engineering, vol. 370, p. 012061, 2018.
23. S. Pavitra, S. Lavanya, and S. A. Khan, "Estimation of Stability Derivatives in Newtonian Limit for Oscillating Cone Estimation of Stability Derivatives in Newtonian Limit for Oscillating Cone," 2018.
24. Asha Crasta, S. Pavitra and Khan S. A., 2016,"Estimation of Surface Pressure Distribution On a Delta Wing with Curved Leading Edges in Hypersonic/Supersonic Flow," International Journal of Energy, Environment and Economics, Vol. 24, Issue No.1, pp. 67-73, e-ISSN: 2349-7688.
25. Aysha Shabana, Renita S Monis, Asha Crasta and Khan S. A., 2018, "Effect of semi vertex angle on stability derivatives for an oscillating cone for the constant value of specific heat ratio," International Journal of Engineering & Technology, Vol. 7, Issue No., pp. 386-390.
26. S. A. Khan, A. Aabid, and C. A. Saleel, "CFD Simulation with Analytical and Theoretical Validation of Different Flow Parameters for the Wedge at Supersonic Mach Number," International Journal of Mechanical and Mechatronics Engineering, no. 01, 2019.
27. R. S. Monis, A. Crasta, and S. A. Khan, "An Effect of Sweep Angle on Roll Damping Derivative for A Delta with Curved Leading Edges in Unsteady Flow," International Journal of Mechanical and Production Engineering Research and Development, vol. 9, no. 2, pp. 361–374, 2019.
28. M. Bashir, S. A. Khan, L. Udayagiri, and A. Noor, "Dynamic Stability of Unguided Projectile with 6- DOF Trajectory Modeling," in 2017 2nd International Conference for Convergence in Technology (I2CT, 2017, pp. 1–8.
29. F. Electron, L. Concept, and L. Alamos, "Chaos in Wraparound Fin," Journal of Guidance, vol. 21, no. 2, pp. 354–356, 1996.
30. W. Asrar, "Chaos in WAF projectile motion TX wraparound fins," AIAA Journal of Guidance, Control & Dynamics, Vol. 21, no. 2, pp. 354-356, March 1998, https://doi.org/10.2514/2.7607